International Conference on Space Optics—ICSO 2004

Toulouse, France

30 March–2 April 2004

Edited by Josiane Costeraste and Errico Armandillo

Laser damage test bench for space optics

Wolfgang Riede, Paul Allenspacher

esa icso proceedings cnes

International Conference on Space Optics — ICSO 2004, edited by Errico Armandillo, Josiane Costeraste, Proc. of SPIE Vol. 10568, 105681X · © 2004 ESA and CNES
CCC code: 0277-786X/17/$18 · doi: 10.1117/12.2307975

LASER DAMAGE TEST BENCH FOR SPACE OPTICS

Wolfgang Riede[(1)], Paul Allenspacher[(2)]

[(1)]German Aerospace Center (DLR), Pfaffenwaldring 38 – 40, 70569 Stuttgart, Germany,
Phone: ++49-711-6862-515, E-Mail: Wolfgang.Riede@dlr.de
[(2)]German Aerospace Center (DLR), Pfaffenwaldring 38 – 40, 70569 Stuttgart, Germany,
Phone: ++49-711-6862-466, E-Mail: Paul.Allenspacher@dlr.de

ABSTRACT

At the German Aerospace Center in Stuttgart a laser damage test bench is run to evaluate damage thresholds of various optical components. The system setup is based on the current ISO standards 11254 [1-3] for single shot and multiple pulse operation. The laser damage test bench contains two repetitively pulsed laser sources, a Ti:Sapphire and a Nd:YAG laser, operating at wavelengths of 775 nm and 1064 nm, respectively. Harmonic wavelength converters to the visible spectral range are available. Both lasers are supplying the same damage testing rig. Online damage assessment techniques like sensitive scatter probe monitoring and video microscopy monitoring are used. The system is suited and has been tested extensively in the past for dielectric coated optics like beam turning mirrors, reflectors and windows, nonlinear optical components, semiconductors, and laser crystals. The damage test bench is located in a class 10,000 cleanroom environment under a laminar flowbox providing an additional isolation factor of $>10^3$. The tests can also be performed in sealed optical compartments in partial vacuum and under long term irradiation conditions. All experiments are supported by theoretical simulation of laser-material interactions, down to the sub-ps timescale [4].

1. INTRODUCTION

Space optics being part of a laser system require stringent product assurance tests for space qualification. To develop a breadboard unit, which has to be subjected to tests under the corresponding operative conditions (surface contamination under long term operation in closed compartment, temperature cycling, (partial) vacuum etc.), initial damage values of all utilized optical components have to be taken into account for system layout. Especially the relevant damage thresholds have to be known, such that the optics can be operated at de-rated levels. In the past, de-rating factors of 25% have been proven to be useful [5].

2. LASER SOURCES

Damage testing requires highly stable laser sources and the ability to monitor each laser pulse accurately. The laser sources, which are part of the test bench, were extensively characterized and are described below. The pulse to pulse energy stability is as stated in Tab. 1b and 2b, respectively. A long term drift of the pulse energy is actively compensated for both lasers.

2.1 Ti:Sapphire laser system

The pulse generation of the Ti:Sapphire laser (Clark CPA 1000) is based on the chirped pulse amplification (CPA) principle. A schematic drawing of the laser is shown in Fig. 1. A frequency doubled fiber ring laser (SErF), operating at a wavelength of 1550 nm, is used as the seed laser source providing sub-ps pulses at 775 nm wavelength. After passing the stretcher, the seed laser is fed into a Ti:Sapphire regenerative amplifier. A $\lambda/2$ wave plate-polarizer combination is used as a variable attenuator. By tuning of the compressor, the FWHM pulse duration can be set to values ranging between 150 fs and 5.5 ps. Blocking of the seed laser results in the emission of 10 ns pulses from the regenerative amplifier. Pulse energies of up to 600 µJ can be attained with smooth Gaussian far field beam profile (Fig.2). The laser pulse duration is inferred from autocorrelation traces. A $(\text{sech})^2$ pulse shape is assumed for the determination of the pulse widths t_p.

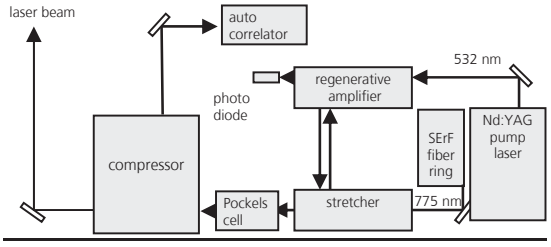

Fig. 1 Ti:Sapphire laser system setup.

The Ti:Sapphire laser system characteristics are summarized in Tab. 1a and 1b.

center wavelength	775 nm
maximum repetition rate	1 kHz
maximum pulse energy	< 0.6 mJ
pulse duration, seeded / unseeded	0.15 – 5.5 ps / 10 ns
pointing stability (long term)	< 10 µrad/h
polarization	parallel
beam quality	$M^2 < 1.5$
linewidth (FWHM)	8 nm

Tab. 1a Ti:Sapphire laser specifications.

repetition rate	+/- 0.05 %
pulse to pulse energy stability	+/- 6.25 %
pulse to pulse spatial profile stability	+/- 1.3 %
pulse to pulse temporal profile stability	+/- 14.6 %

Tab. 1b Ti:Sapphire laser pulse to pulse error budget.

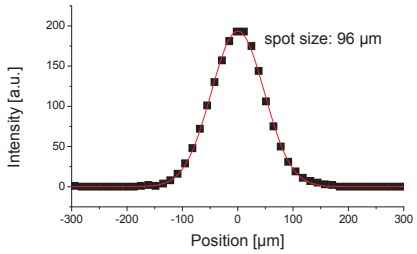

Fig. 2 1-dim far-field beam profile of the Ti:Sapphire laser. The solid line is a Gaussian fit to the measured intensity profile (squares).

2.2 Nd:YAG laser

A second laser source operated as part of the test bench is a Coherent Infinity 40-100 Nd:YAG laser, which delivers a single longitudinal mode laser beam of high spatial quality at a wavelength of 1.064 µm. Due to single longitudinal mode operation it has a small linewidth of 250 MHz.
The Nd:YAG laser characteristics are summarized in Tab. 2a and 2b. The system fulfils the maximum percentage variation of the laser parameters specified in the ISO standard 11254.

wavelength	1064 nm
maximum repetition rate	100 Hz
maximum pulse energy	up to 600 mJ
pulse duration (FWHM)	4 ns
pointing stability (long term)	20 µrad/h
polarization	parallel
beam quality	$M^2 < 1.5$
linewidth	< 250 MHz / < 1 pm

Tab. 2a Nd:YAG laser specifications.

repetition rate	+/- 0.001 %
pulse to pulse energy stability	+/- 1.3 %
pulse to pulse spatial profile stability	+/- 3.3 %
pulse to pulse temporal profile stability	+/- 5 %
pulse to pulse pointing stability	+/- 10 µrad

Tab. 2b Nd:YAG laser pulse to pulse error budget (data are valid for pulses of 300 mJ, t_p = 4 ns and 100 Hz operation).

3. DAMAGE SETUP

The typical multipulse laser damage setup is shown schematically in Fig. 3 and as a photograph in Fig. 4. From the main beam delivered by the laser source, two reference beams are split off to monitor energy and near field beam profile (camera 2). A lens of selected focal length (e.g. 0.5 m) focuses the radiation onto the sample front surface. An identical lens is used to monitor the far field distribution (camera 1). The distance between the focusing lens and the CCD camera chip is adjusted for optimum roundness of the far field distribution. The camera based beam profile measurements have to be confirmed before the experiment with a knife-edge beam scan in the sample front surface plane. The distance between the focusing lens and the sample front surface must be adjusted accordingly. An intensity stabilized, chopped HeNe laser is tuned exactly to the position of the sample surface onto which the damaging laser pulses are focused. The modulation of the HeNe laser allows for an improved signal to noise ratio by implementing lock-in techniques. An opaque aperture centered on a second lens, blocks the HeNe laser beam which is specularly reflected off the sample front surface. Hence, only scattered light reaches the diode. All data (position, accumulated energy, beam profile, scatter light, number of pulses) are stored using a PC for later retrieval and analysis. The resolution of the used data acquisition hardware is within the limits required from ISO 11254 (pulse energy measurement uncertainty < 5 %, temporal resolution < 0.1 * t_p, spatial resolution < +/- 1.5 % of beam diameter). A flowbox, mounted above the laser damage setup, provides a laminar flow of filtered air of high quality (max. 10 particulates / cubic foot).

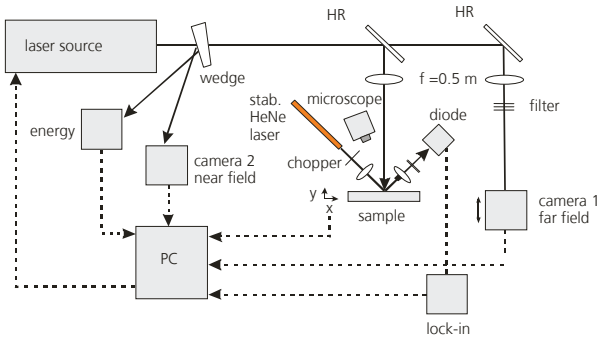

Fig. 3 Laser damage setup.

Fig. 4 Photograph of the laser damage setup with flowbox (above).

4. PRETEST EVALUATION, CLEANING, AND HANDLING OF OPTICS

Prior to damage testing, the optical components are inspected with a Nomarski microscope at a magnification of at least 100X. This evaluation identifies any preexisting flaws in the optical surface that would otherwise be included in the posttest damage assessment. The pretest optical evaluation also provides a means of assessing the cleanliness of the optical surface prior to testing. If the optic requires further cleaning, a drag-wipe cleaning procedure is used. With this procedure, the optical surface is cleaned with a lint-free cloth and spectroscopic grade methanol and/or acetone.
At all times during the test procedure, the optics are handled by the edges wearing finger cots to prevent accidental contact to the optical surface. The samples are inspected and irradiated in a class 10 cleanroom environment. In general, these handling and storage measures ensure that the test specimens have not been influenced by the laboratory environment so that an unbiased estimate of the laser induced damage threshold (LIDT) is obtained.

5. SAMPLE IRRADIATION METHOD AND EVALUATION

The samples will be irradiated after a laser warm up period of approximately 1 hour. The irradiation can be performed over an extended period of time (several hours) at the given laser repetition rates (c.f. Tab.1, 2) by focusing the laser beam with a suitable lens. The irradiation centers on the sample are usually equally spaced in an array with a periodicity of 1 mm. In general, the grid spacing is selected such that debris emission from one site will not interfere with adjacent sites (ISO 11254 recommends a spacing of 3 X beam radius). The sample surface has to be adjusted parallel to the movement of the x-y translation stage. The samples can be exposed to a permanent dry nitrogen flush. The occurrence of damage is monitored online with scatter probe techniques (c.f. section 3), which allows for an immediate interruption of the irradiating pulse sequence. The scatter probe technique usually discriminates front and back surface damage. After irradiation, the occurrence of damage is always verified by subsequent inspection with a Nomarski differential interference contrast (DIC) microscope.

beam diameter in target plane, $1/e^2$:	200 µm
number of pulses per site:	10^4
total number of sites per specimen:	> 200
angle of incidence:	0°
arrangement of test sites:	equally spaced
distance between sites:	1 mm

Tab. 3 Summary of typical damage test parameters.

After the inspection, the result of the multiple pulse irradiation is a file of data points, containing the fluence values and the number of pulses at which damage has occurred. The data have to be processed according to the ISO standard 11254 leading to probability damage curves and characteristic damage curves. Examples are detailed in the following section 6.

6. EXPERIMENTAL RESULTS

In this section, the results of single shot and multiple pulse damage tests are explained using the results of recent investigations [6, 7].

6.1 Damage probability plot

A typical damage probability plot, derived from AR coated beat-barium borate (BBO) is depicted in Fig. 5 for a pulse number N = 200, applied to 121 different sites at a pulse duration of 1 ps. The plot shows the probability of damage as a function of applied fluence. The intersection of a linear fit through the data points with the abscissa defines the LIDT value which is 1.58 J/cm^2. The length of the shown error bars is inversely proportional to the statistical significance in the corresponding fluence interval. Only front surface damage is taken into account for this evaluation.

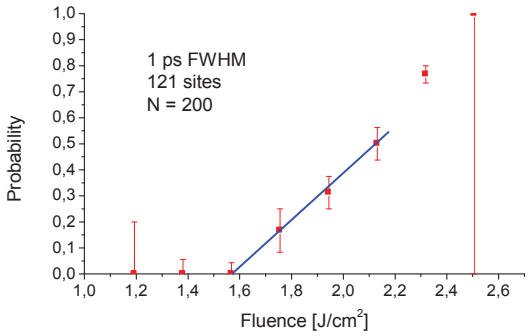

Fig. 5 Damage probability curve of AR coated BBO (775 nm, pulse duration t_p = 1 ps, 121 sites, N = 200 shots/site).

6.2 Characteristic damage curves

The characteristic damage curve has to be extracted from several probability plots. Fig. 6 shows the result of measurements of an HR mirror coated for a wavelength of 775 nm. Displayed are the 0 %, 10 %, 50 %, and 90 % curves attained form probability plots at different pulse numbers per site. The pulse number N in the plot ranges from N = 2 to 10 000. It is evident that the LIDT value is decreasing with increasing number of pulses per site. The dependence of the LIDT on N is due to incubation effects, i.e., the generation of defect centers. These defect centers induce local absorption with a subsequent rise in temperature or stress. The

processes are material specific and not yet fully understood [8].

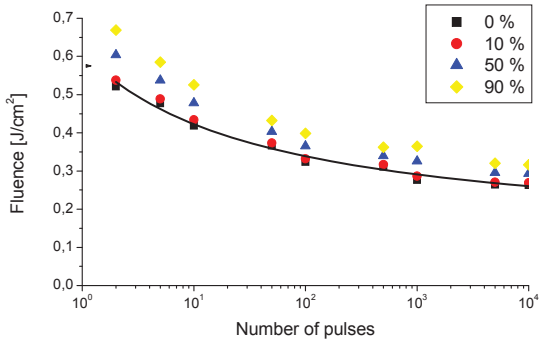

Fig. 6 Characteristic damage curve of fused silica substrate, coating HR @ 780 nm, HT @ 532 nm, t_p = 150 fs.

7. EXTRAPOLATION

Based on the measured characteristic damage curves of optical components, an extrapolation to higher number of pulses can be performed using the formula (1) [2]:

$$F(N) = F_\infty + (F_1 - F_\infty)/(1+\log(N)/\Delta) \qquad (1)$$

where F_1 and F_∞ are the damage fluences for pulse numbers N = 1 and N = Infinity and Δ is a fit parameter.
When applying this formula to the results shown in Fig. 6, a safe operation zone can be denoted for the tested optical component. This safe operation zone is visualized in Fig. 7 as the grey area under the fitted curve. In the limit of an infinite number of pulses (called the endurance limit), the damage fluence is found in case of the example of HR coated fused silica: F_∞ = 0.12 J/cm² whereas the single pulse threshold is F_1 = 0.6 J/cm².

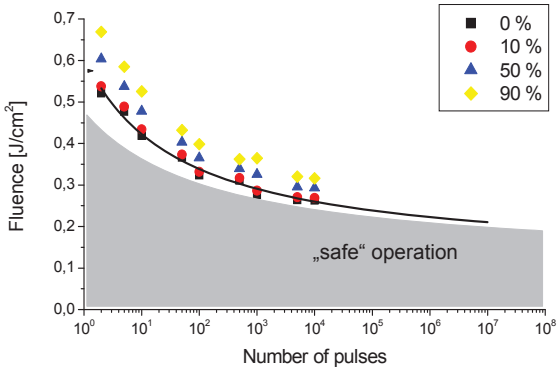

Fig. 7 Safe operation of optical components for fluence values below characteristic damage curve. (experimental data c.f. caption of Fig.6).

8. SAMPLE INSPECTION

Damage detection is being done using a light microscope having Nomarski-type DIC setup with a magnification of 100X – 150X (c.f. Fig. 8). Damage is then defined as any permanent surface modification being visualized with the mentioned equipment.

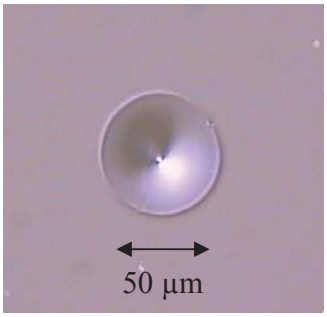

Fig. 8 Nomarski DIC micrograph of back surface damage of periodically poled $LiNbO_3$ at a wavelength of 1.06 µm, F = 6.2 J/cm², t_p = 4 ns.

High resolution 3-dimensional images of the irradiated surface are attained from an atomic force microscope (SIS UltraObjective, c.f. Fig. 9), which has a scanning range of 40 X 40 µm².

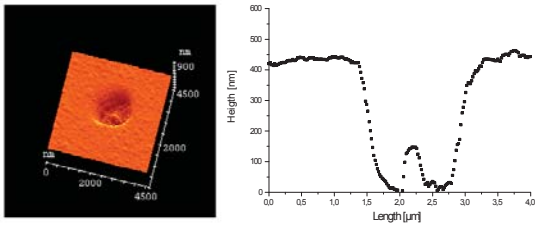

Fig. 9 Topography of front surface damage of AR coated BK7 glass sample.

A white light interference microscope (ATOS Micromap 512) is utilized for the inspection of larger surface areas. Both instruments are very useful for the analysis of laser damage processes.

9. SUMMARY AND OUTLOOK

In this paper the capabilities of the laser damage test facilities at DLR Stuttgart are comprehensively summarized. The test bench is suited for measuring multiple pulse damage thresholds for an in principle unlimited number of pulses as the system has a stabilized energy output and is fully automated. Various optical components can be tested like beam turning mirrors, reflectors and windows, nonlinear optical components, semiconductors, and laser crystals. Characteristic damage curves are evaluated according to ISO 11254 2.0 Scaling of the characteristic damage curve to very high pulse numbers delivers useful product assurance data.

Hence, the system can provide initial damage threshold data for the layout of satellite-based pulsed laser systems.
Future improvements will be concentrating on achieving ISO certification. Furthermore, contamination-induced damage effects in sealed laser systems will be taken into account.

10. ACKNOWLEDGEMENTS

We kindly acknowledge the support of Bernd Hüttner concerning the theoretical description of laser damage processes and the technical support of Ralf Bähnisch (both DLR Stuttgart).

11. REFERENCES

1. ISO/FDIS 11254-1:2000, *Lasers and laser-related equipment - Determination of laser-induced damage threshold of optical surfaces, Part 1: 1-on-1 test*, 2000.

2. ISO/FDIS 11254-2:2001(E), *Lasers and laser-related equipment - Determination of laser-induced damage threshold of optical surfaces, Part 2: S-on-1 test*, 2001.

3. ISO 11254-3, *Lasers and laser-related equipment - Determination of laser-induced damage threshold of optical surfaces, Part 3.2 Certification of the laser power handling capabilities*, to be published.

4. Huettner, B., *Calculation of the damage thresholds of semiconductors*, 35. Annual Symposium on Optical Materials for High Power Lasers, Boulder, CO, 2003.

5. Hovis, F et al., *Space-based laser design*, Proc. SPIE 3091, 93-96, 1996.

6. Allenspacher, P., Baehnisch, R., Riede, W., *Multiple ultra short pulse damage of AR coated beta-barium borate*, 35. Annual Symposium on Optical Materials for High Power Lasers, Boulder, CO, 2003.

7. Starke, K, Riede, W, Allenspacher, P, et al., *Results of a Round Robin experiment in multiple-pulse LIDT measurement with ultrashort pulses*, 35. Annual Symposium on Optical Materials for High Power Lasers, Boulder, CO, 2003.

8. Koldunov, M.F. et al., *Multishot laser damage in transparent solids: theory of accumulation effects,* SPIE 2428, 1995.